

Novel TiO₂ Microstructures for Low Cost Dye Sensitized Solar Cells

P. Fuierer¹, A. Gueye², A. Varghese³, B. Roy⁴

¹Dept of Materials & Metallurgical Eng., New Mexico Institute of Mining & Tech., Socorro, NM87801 (USA)
phone: (575) 835-5497 email: fuierer@nmt.edu

²Plextronics, Inc., Pittsburgh, PA 15238 (USA)
phone: (412) 423-2039 email: agueye@plextronics.com

³CIRIMAT INP-CNRS Institute National Polytechnique de Toulouse, 31030 Toulouse (France)
phone: (+ 33) 5 34 32 34 53 email: AneeshaMary.Varghese@ensiacet.fr

⁴Chemical Engineering Dept., New Mexico Institute of Mining & Technology, Socorro, NM 87801 (USA)
phone: (575) 835-5937 email: broy@nmt.edu

Abstract A critical component of the dye sensitized solar cell (DSSC) is the nano-structured wide bandgap semiconductor (typically TiO₂). The particle size, crystal structure, orientation, and scale of interconnected porosity are all critical to cell performance. In our lab, we have engineered and produced ceramic pastes including a hierarchy of nano- to micron-sized particles of varying morphologies and texture which yield novel, hybrid microstructures. We assert that while the nano-material provides the surface area, the micro particles provide conduits for easier diffusion of photo-generated electrons through the titania and also a pore structure for percolation of dye and electrolyte, giving enhanced photo-current and power output. The pastes also are of practical benefit, as they avoid shrinkage cracks during drying, and result in high quality thick films.

Keywords dye sensitized solar cells (DSSC), titanium dioxide, hierarchical microstructures, nanomaterials

Introduction

The vision of low cost, ubiquitous solar power systems requires a paradigm shift in photovoltaic (PV) materials and manufacturing. Any new energy source must use abundant, non-toxic materials. It must be produced in a scalable process requiring low capital investment. The goal of our work is to conduct the science required toward the design of a material coating system which can be applied on site by skilled labor that will generate electricity for a fraction of current PV cost. The technology of focus is the dye sensitized solar cell (DSSC), a hybrid organic/inorganic device with proven efficiencies of 10%, and estimated costs at just 10 to 20% of state of the art silicon devices [1-3]. The DSSC is a 3rd generation PV just beginning commercialization [4-5].

The role of the dye (typically bipyridyl complexes of Ru²⁺) in DSSC is to absorb visible light, pump an electron (*e*⁻) into the wide band gap semiconductor of the anode, and accept an *e*⁻ from the redox couple (I⁻/I₃⁻) to repeat the cycle [2]. One limitation of the DSSC is the tortuous *e*⁻ percolation path between weakly linked nano-anatase particles giving high internal resistance and low current output. Li *et al.* [6] has recently verified, via impedance

spectroscopy and numerical simulation, that *e*⁻ transport and recombination dominate operation of DSSC, and an optimal bimodal distribution of nanoparticles can benefit performance. Several research groups (examples given in references [7-10]) have taken the approach of growing oriented TiO₂ and ZnO nano-rods or -tubes to enable easy transport of *e*⁻s to the anode, however; the height of nanopillar arrays is limited to a few tens of nanometers, which limits the amount of light absorption in the cell. In addition, growing very large areas in an economical fashion is difficult to envision.

Percolation of electrons is not the only issue. Diffusion of the electrolyte, whether the typical low viscosity organic solvent type or newer higher viscosity polymers, to and from the dye-covered TiO₂ surfaces is critical to maintaining high current. In the case of iodine solutions, I₃⁻ must quickly diffuse from the surface during operation to reduce recombination events and the undesirable dark current.

An optimized film structure has been shown to be one containing meso-porous channels aligned perpendicular to the substrate [11], which again justifies the fervor over using aligned nano-tubes or rods. A more novel and potentially practical idea was recently reported where an "inverse opal" microstructure was produced from commercially available titania nanoparticles giving DSSC with efficiencies greater than 4% [12].

It has been suggested that optical effects resulting from the nano-structured semiconductor provide opportunities for increasing the total efficiency of DSSC [13-18]. As in the well known textured single crystal Si solar cell, surface roughness can reduce specular reflectance. Enhanced internal light scattering may increase the average photon path length, increasing the probability for photon capture by the dye, an idea similar to the dependence of opacity of paint coatings and paper on multiple scattering from large numbers of particles comparable to wavelength [20]. Moreover, light should be absorbed over the widest possible range of wavelengths, and interaction of the dye with varying surfaces may

broaden the absorption. Recent experimental work by Cao *et al* [21] at the University of Washington has shown that admixtures of poly-disperse, submicron ZnO aggregates (popcorn style) made of primary nano-crystallites can enhance DSSC efficiency. Making anodes from electro-spun nano-titania fibers is another recent approach to increase photon harvesting and electron transport, with potential for scale-up [22,23].

Our premise is that DSSC is an example of a (photochemical-electrical) device which can benefit from a heterogeneous, hierarchical mixture of TiO₂ particle sizes and morphologies. The requisite heterogeneity may preclude the use of exotic material growth techniques and instead favor the use of simple, engineered mixtures of particles and cost effective thick film deposition.

Objective and Approach

Recognizing the benefits of simple coating procedures to reduce production costs, we set out to develop TiO₂ - ceramic pastes that could be very easily applied by casting, rolling or other thick film process technologies [24]. These pastes included both nano and micron-sized particles of varying morphologies in order to yield novel, hybrid microstructures. Figure 1 shows schematics of two of the microstructures that we have attempted to fabricate and incorporate into the DSSC. While nanocrystalline anatase provides the high surface area, rutile needles and/or hollow glass microspheres with dense TiO₂ thin film provide enhanced scattering and conduits for easier percolation of photoelectrons to the electrode. A titania sol is used to “chemically sinter” the particles.

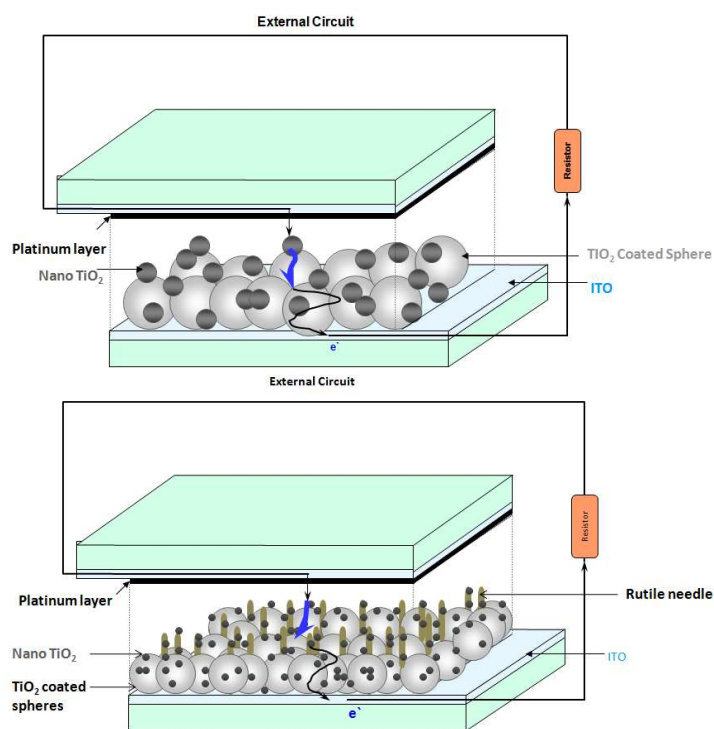


Fig. 1. a) Schematic DSSC with photoanode made of nano-crystalline anatase and TiO₂-coated glass microspheres, “chemically sintered” by sol-gel. b) Proposed photoanode including acicular rutile with “stand-up-texture”.

Experimental Procedure

For the purpose of comparison, films referred to as type A were prepared using only nanoanatase (*a*), according to a recipe commonly used to build DSSCs [25]. This formulation calls for 6g of Degussa P-25 powder, 1.5 ml of ethylene glycol (EG) and 9ml of a nitric acid solution (HNO₃/H₂O). Our novel pastes included both *a* and micron size particles, uniformly mixed with a titania sol as the liquid vehicle. The sol was prepared by dissolving titanium isopropoxide in ethanol with acetic acid as a chelating agent, and hydrolyzing with H₂O₂. Details are given in reference [26]. Films produced from a mixture of the sol vehicle and *a* are referred to as SGA (*tn* and *tk* refer to thin and thick respectively). SGAR refers to formulations with commercially available acicular rutile, *r*, (FTL300, Ishihara Sangyo Inc.) as an additive. Two different *a* to *r* mass ratios were used, 1:1, and 7:1 (the latter corresponding to the ideal case of a single layer, uniform coverage of *a* on *r*). Titania spheres, *ts*, were another type of additive produced by dissolving titanium isopropoxide in isopropanol and acetic acid and spray dried using a Buchi B-290 Mini Spray dryer (details found in ref [27]). Film SGATS is one of the film types containing these micro-particles. The last type of additive is called coated spheres, *cs*. These were prepared by treating glass microspheres (SID-350Z, Trelleborg, Inc.) in the titanium sol above, filtering, hydrolyzing in air, suspending in ethanol, and spray drying using the Buchi B-290 [27]. Corresponding films include SGACS. A total of 25 different formulations involving various combinations of these TiO₂ particles were prepared and investigated. For brevity sake, we will refer to only a dozen in this discussion (Table 1).

Paste preparation began with mixing 18 vol% *a* with ethylene glycol (to control viscosity, plasticity and film shrinkage), followed by addition of titania sol, and then micro-titania of the sorts described above. Films were deposited onto borosilicate glass slides with a fluorine doped tin oxide conductive coating (TEC 15, Hartford Glass, Inc.) using a simple casting procedure with a smooth glass rod. Either 30 μm or 60 μm thick masking tape was used to define the electrode film area (1.7x1.7 cm) and thickness. A humidity chamber was used to control the drying time in order to minimize shrinkage cracks. Films were then annealed at 450°C for 30 min.

For solar cell preparation, crack-free titania films were soaked for 24 hrs. in a 3.10 x10⁻⁵ M ethanol solution of N719 ruthenium 535-bis TBA dye (Solaronix, Inc.), rinsed in ethanol, and allowed to dry in a dry box. Counter electrodes were produced by sputter coating a Pt layer approximately 80 nm thick onto another conductive glass slide, followed by a 450°C anneal for 15 min. The dyed anode and Pt counter electrodes were then placed face to face with a either a 30 μm or 60 μm thick spacer around the perimeter, and secured with a clamp. Immediately prior to testing, a drop or two of the redox couple I₃/I⁻ electrolyte (0.5M KI/0.05M Iodine in ethylene glycol) was introduced at the edge and drawn in by capillary action to wet the entire cell electrode.

The solar cell performance was characterized by measuring the I-V curves when irradiated with simulated AM 1.5 light of power density $P_{in} = 100 \text{ mW/cm}^2$ (Sciencetech 1.6KW Solar Simulator with KeithleyMeter). The Sciencetech SSI-VT software automatically provides parameters of interest including open circuit voltage, V_{oc} , short circuit current, I_{sc} , power curve, maximum power, P_{max} , and fill factor. Measurements were made at exposure times of 1 min, 5 min, and 10 min.

Multipoint BET surface area of powders and mixtures was performed using a Nova 2200 (Quantachrome Instruments) and ultra high pure N_2 gas. Approximately 0.035g of sample was used and degassed for 2 hrs at 150°C . Imaging of powders and film samples was done on a field emission SEM (Hitachi S-800) after coating with a thin layer ($\sim 15 \text{ nm}$) of evaporated carbon. A Dektak contact profilometer (Veeco) was used to measure thickness and roughness of the films using a slow scan speed and 5mm scan length.

Results & Discussion

Figure 2 shows the nature of the TiO_2 particles prior to admixture. Measured specific surface areas for nano-anatase (*a*), acicular rutile (*r*), spray dried titania spheres (*ts*), and titania-coated glass microspheres (*cs*) are 56.1, 6.0, 10.8, and 8.3 m^2/g respectively. Following 500°C anneal, these values change to 48.3, 6.0, 7.0, and 10.8 m^2/g . The increase in SA for the *cs* is interesting to note.

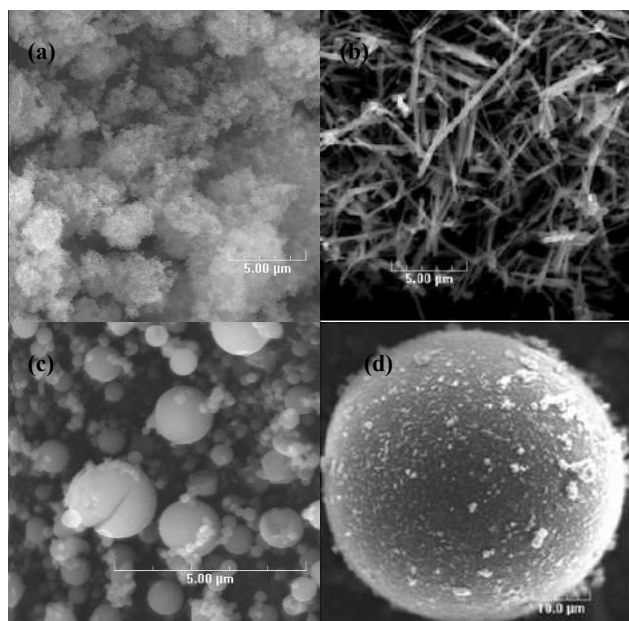


Fig. 2 SEM images of a) nano-anatase (Degussa P-25), b) acicular rutile (FTL-300, Ishihara Sangyo), c) spray dried titania spheres, and d) titania coated glass microspheres.

Table 1 summarizes the physical properties of films produced from the different formulations. Measured BET surface area (SA_m) and pore characteristics (radius and volume) are given for a few mixtures, as well as surface areas predicted via weighted calculations (SA_c). In this calculation, the sol-gel titania is ignored for two reasons: 1. the relatively small amount, and 2. the nano-titania

resulting from the sol is known to be very small and reactive [26], and likely disappears during anneal due to Ostwald ripening of the larger particles. Again of note is the increase in specific surface area of the formulation containing *cs* from 27.7 to 38.0 when the sample is annealed. Also note the increase in the average pore radius with annealing.

Figure 3 illustrates the variety of microstructures produced. 3(a) shows that the anatase does not uniformly decorate the rutile, but rather agglomerates to some extent. No attempt at orientation of rutile needles was made in this sample, and none is seen. 3(b) shows how the titania spheres have collapsed and fused to one another along with *a* and titania sol particles. 3(c) shows a microsphere embedded in *a*. 3(d) shows two neighboring glass microspheres, enveloped in a mix of *a* and *r*. There appears to be a rutile crystallite in between which has grown to a rather large size, an uncommon occurrence.

Table I. Physical characteristics of TiO_2 films

		t	R	SA_c	SA_m	r_p	V_p
		μm	μm	m^2/g	m^2/g	nm	cc/g
A	A annealed	13.9	.71		56.1 48.3	16	.14
1	SGA-tn	6.64	.47	56.1			
2	SGA-tk	14.1	.72	56.1			
3	SGR			6.0	6.01	7.5	.14
4	SGAR 1:1 annealed	18.4	1.1	31.1 27.2	31.3 18.4	15 17	.07 .10
5	SGAR 7:1	18.2	1.3	49.8			
6	SGTS	6.2		10.8			
7	SGATS	15.8	.79	50.4			
8	SGARTS	19.5	1.5	45.5			
11	SGCS	31.7	2.3	8.3			
17	SGACS	41.8	3.8	50.1			
18	SGARCS annealed	44.7	5.6	45.2 35.5	27.7 38.0	15 19	.97 .24
24	SGARTSCS	44.9	6.0	41.8			

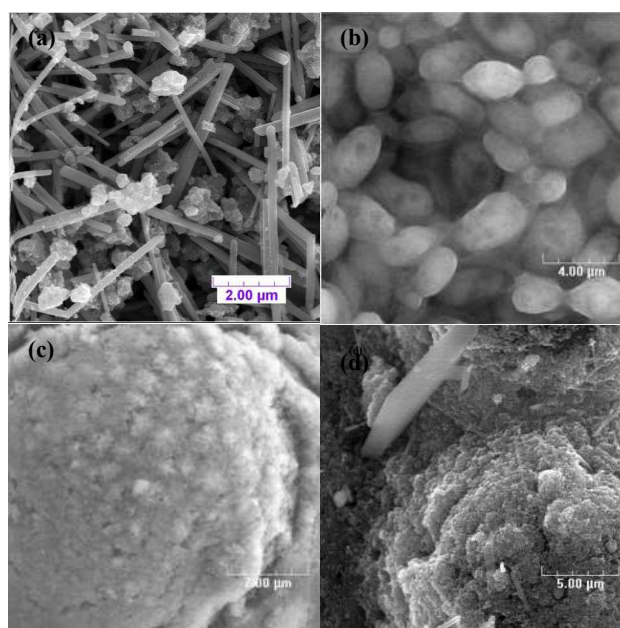


Fig. 3. Electron micrographs of films a) SGAR1:1, b) SGATS, c) SGACS, and d) SGARCS.

The I-V responses of two experimental films are shown in Fig 4. Generally, films showed decay in output with time, very pronounced in the case of SGA-tn, which was similar to standard film A. Stability over time is a well known challenge with DSSCs, and can be attributed to loss of liquid electrolyte and/or UV photodegradation of the dye. Loss of the liquid electrolyte by leakage and/or evaporation of the solvent can be addressed by proper sealing, but perfect sealing can be difficult. Degradation can be addressed by UV filtering and chemical stabilizers [28], but this introduces additional complexities. We chose to run these sets of comparative experiments by keeping preparation and exposure times consistent.

In addition to increasing overall power output, incorporation of acicular rutile in (SGAR 7:1) appeared to significantly stabilize the response with exposure time, as did other micro-particles. Table II compares the maximum power output (P_{max}) for a dozen experimental cell-types. Values shown are averages of three cells made in identical fashion. While the presence of nanocrystalline anatase is required for photovoltaic response (ie null response from SGR and SGTS), addition of micro-particles almost always improves performance. The best cells were those containing either spray dried or coated glass microspheres (which themselves contain *a* as a coating). Fig. 5 illustrates the improved performance of the hierarchical composite photo-anodes over the standard A type. The P_{max} and corresponding efficiency are up to 5 times that of the standard cell comprising only *a*. Most of the improvement comes by large increase in photocurrent.

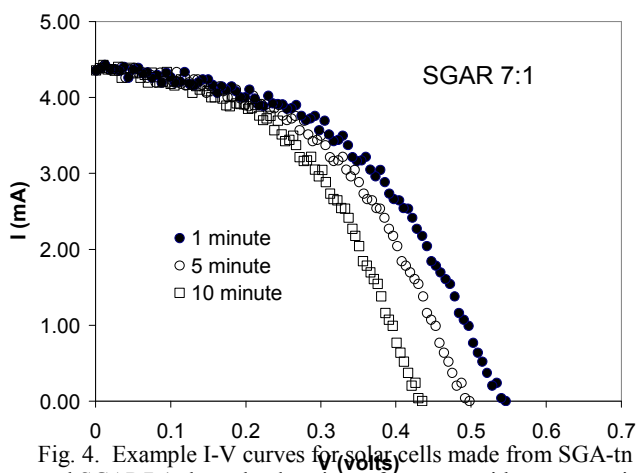
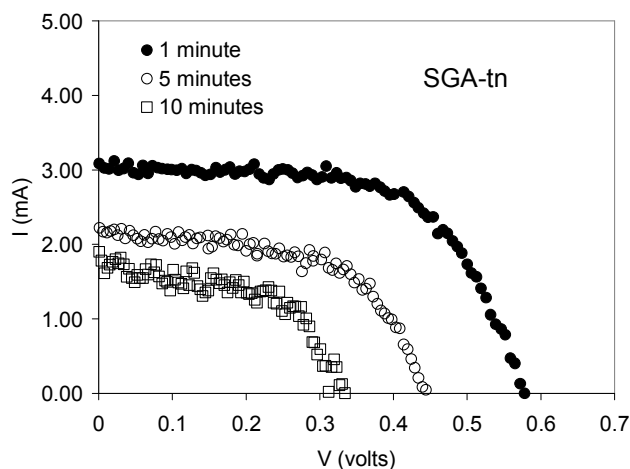


Fig. 4. Example I-V curves for solar cells made from SGA-tn and SGAR7:1 show the drop in performance with exposure time.

The beneficial effects of *cs* can be partially explained by comparing pore characteristics (Table I). Annealed SGARCS has a larger average pore radius (19nm), and significantly larger pore volume (0.24cc/g) than the simple anatase film (16nm and 0.14cc/g respectively). Opening up a larger amount of meso-porosity allows for better diffusion of dye and electrolyte, as discussed earlier. SGAR1:1 actually yielded decreased pore volume, perhaps due to more efficient space filling with *a* and *r*, and therefore little performance improvement.

It is important to note that the highest efficiencies measured (at 1 min exposure) in this study were modest (ca 1.2%). This is attributed to several factors: 1. Time degradation mentioned above. 2. Dye selection. 3. Non-optimized counter-electrode. 4. Non-optimized electrolyte, which are all critical to maximize performance of the DSSC device. Our intent was to explore the influence of the titania anode microstructure, and experiments yielded repeatable results.

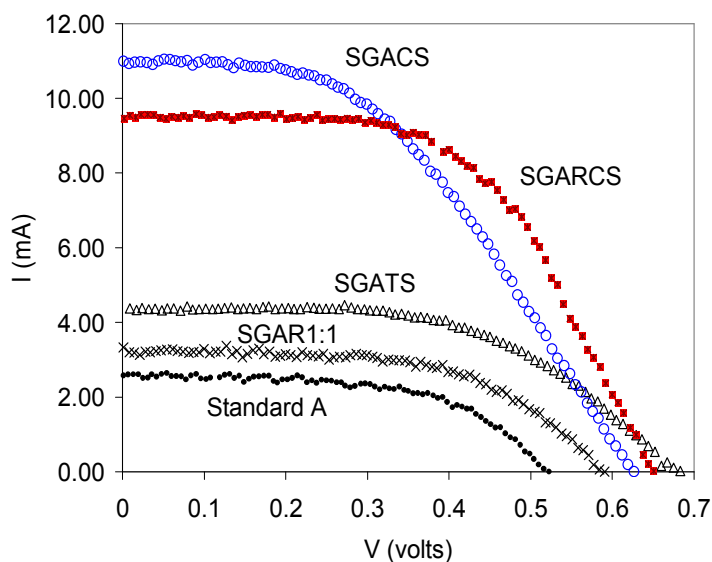


Fig. 5. I-V response of DSSCs made with hierarchical microstructured anodes (shown in Fig. 3), compared to a standard A photoanode. Measurements were made under simulated solar irradiation (AM1.5G, 100 mW/cm²) at 1 minute exposure time.

Table II. Photovoltaic parameters (average of 3 cells)

	exposure→	1m		5m			
		V_{oc}	I_{sc}	P_{max}	V_{oc}	I_{sc}	P_{max}
		mV	mA	mW	mV	mA	mW
A	A	.54	2.4	.72	.42	2.4	.47
1	SGA-tn	.60	2.8	.99	.42	2.1	.46
2	SGA-tk	.60	3.3	1.3	.48	2.7	.73
3	SGR	-	-	-	-	-	-
4	SGAR 1:1	.59	3.09	1.11	.54	3.4	1.0
5	SGAR 7:1	.63	4.0	1.43	.54	4.3	1.1
6	SGTS	-	-	-	-	-	-
7	SGATS	.66	5.5	1.86	.59	4.7	1.50
8	SGARTS	.67	8.03	3.15	.58	7.6	2.40
11	SGCS	.45	.956	.31	.32	.96	.17
17	SGACS	.65	9.57	3.14	.52	8.4	2.10
18	SGARCS	.62	8.52	2.85	.52	8.1	2.01
24	SGARTSCS	.64	6.50	2.42	.50	6.5	1.67

It is tempting to search for trends in performance. Fig. 6 plots the P_{\max} vs calculated surface area of the composite photo-anode. Referring back to Table I, the SA_c calculated from weighted contributions using measured SA of untreated powders agreed with that measured for SGAR1:1. On the other hand, the SA_c calculated using SA measured on annealed powders matched the measured SA_m of SGARCS. So both approaches are used in the plot. Although there is uncertainty in the absolute SA values, the trend suggests that strictly higher surface area is not necessarily the answer for highest PV output. Performance is determined by other characteristics as well, such as the nature of the pores and their size distribution, Mie scattering from micro-particles and so on as discussed earlier.

Figure 7 plots P_{\max} vs thickness of the composite TiO_2 anode. The error bars indicate the approximate ranges for the three measured values, generally about $\pm 10\%$. The trend appears to have a positive slope (albeit scattered), discounting the outlier at about $t=30\mu m$ which corresponds to SGCS containing no *a*. This low output is not surprising, as the use of only glass micro-sphere particles yields low SA and significant void space in the film. For hierarchical microstructures, the plot suggests increased performance with thicker films, very different from the typical conclusion when using only mono-dispersed nanoparticles...usually showing decreased performance above about $t=10\mu m$. Of course thicker films (more material) are required to achieve greater surface areas in hierarchical films. We believe that increased number of scattering events and more efficient light trapping is also responsible for this trend. In addition, we observe that heterogeneous large-particle pastes can avoid the typical shrinkage cracks that occur during drying of nano-particulate films, and allow higher quality thick films to be made.

At this point, it is unclear whether the inclusion of larger particles affords more direct transport of electrons through the photoanode as proposed, but the increased photocurrents suggest that it is a possibility. Detailed impedance spectroscopy is required to bear this out.

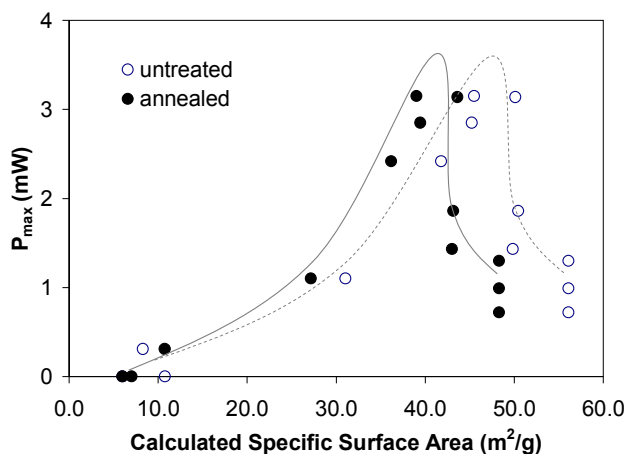


Fig. 6. P_{\max} (1 minute exposure) vs specific surface area of composite TiO_2 photoanodes calculated from surface areas of individual components. The lines are sketched as a visual aid.

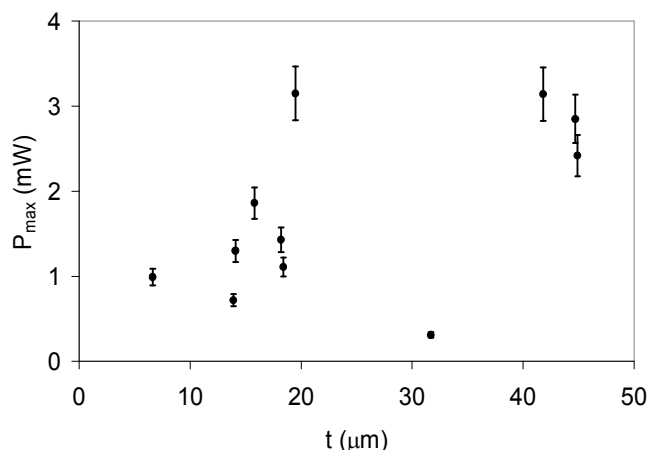


Fig. 7. P_{\max} (1 minute exposure) vs photoanode thickness.

Conclusion

We have demonstrated that the performance of dye sensitized solar cells can be improved significantly by using photoanodes with heterogeneously microstructured titania. Though some progress has been made [29,30], we have not yet succeeded in achieving ideal vertically aligned rutile needles. However this work shows that their inclusion even with random orientation offers improvement. The incorporation of titania-coated glass microspheres is a unique approach which allows good quality thick films and repeatable, high PV output, up to four or five times that of a DSSC made using the standard nano-anatase photoanode. Our results suggest that while total surface area is important, so too is the connectivity of the titania, the nature of the pore network, and the extent of light scattering within the photoanode. Whereas others have supported this conclusion experimentally using designer nanostructures such as nanotubes, we have presented a comparatively simple approach using commercially available materials to create hierarchical structures.

Acknowledgment

The authors acknowledge financial support for this work from the US Dept. of Energy grant # FC26-06NT42854.

References

- [1] B. O'Regan and M. Gratzel, "A low-cost, high-efficiency solar-cell based on dye-sensitized colloidal TiO_2 films", *Nature* 353, (1991) pp.737-740.
- [2] C. Longo and M. DePaoli, "Dye-Sensitized Solar Cells: A Successful Combination of Materials", *J. Braz. Chem. Soc.*, 14 (6) (2003) pp 889-901.
- [3] J. Mazer, "Photovoltaic Technology and Recent Developments with the DOE Solar America Initiative", *Vacuum & Coating Technology* (April, 2008) pp 39-47.
- [4] L. Goncalves, V. Bermudez, H. Ribeiro, and A. Menes, "Dye-sensitized solar cells: A safe bet for the future", *Energy Environ. Sci.*, 1 (2008) pp. 655-667.
- [5] G24 Innovations, Limited, Cardiff, Wales, UK. <http://www.g24i.com>

- [6] X. Li, H. Lin, J. Li, X. Li, B. Cui, L. Zhang, "A Numerical Simulation and Impedance Study of the Electron Transport and Recombination in Binder-Free TiO₂ Film for Flexible Dye-Sensitized Solar Cells", *J. Phys. Chem. C*, 112, (2008) pp. 13744-13753.
- [7] M. Adachi, Y. Murata, I. Okada, S. Yoshikawa, "Formation of Titania Nanotubes and Applications for Dye-Sensitized Solar Cells", *J. Electrochem. Soc.* 150 [8] (2003) G488-493.
- [8] H. Wang, C. Yip, K. Cheung, A. Djuricic, M. Xie, Y. Leung, W. Chan, "Titania nanotube array based photovoltaic cells", *Appl. Phys. Lett.* 89 (2006) 023508-1-3.
- [9] C. Grimes, G. Mor, O. Varghese, M. Paulose and K. Shankar, "A review on highly ordered, vertically oriented TiO₂ nanotube arrays: Fabrication, material properties, and solar energy applications", *Solar Energy Materials and Solar Cells*, 90, (2006) pp. 2011-2075.
- [10] J. Baxter and E. Aydil, "Nanowire-based dye-sensitized solar cells", *Appl. Phys. Lett.* 86 (2005) pp. 053114-1-3.
- [11] M. Gratzel, "Perspectives for Dye-Sensitized Nanocrystalline Solar Cells," *Prog. Photovoltaics* 8 [1] (2000) pp. 171-185.
- [12] L. Qi, J. Sorge, and D. Birnie III, "Dye-Sensitized Solar Cells Based on TiO₂ Coatings with Dual Size-scale Porosity", *J. Am. Ceram. Soc.* 92 [9] (2009) pp. 1921-1925.
- [13] J. Ferber and J. Luther, "Computer simulations of light scattering and absorption in dye-sensitized solar cells", *Sol. Energy Materials & Solar Cells*, 54 (1998) pp. 265-275.
- [14] C. Rockstuhl, F. Lederer, K. Bittkau, and R. Carius, "Light localization at randomly textured surfaces for solar-cell applications", *Appl. Phys. Lett.* 91 (2007) pp.171104-1-3.
- [15] T. Chou, Q. Zhang, B. Russo, G. Fryxell, and G. Cao, "Titania Particle Size Effect on the Overall Performance of Dye-Sensitized Solar Cells", *J. Phys. Chem. C* 111 [17] (2007) pp. 6296-6302.
- [16] G. Rothenberger, P. Comte, M. Gratzel, "A Contribution to the Optical Design of Dye-Sensitized Nanocrystalline Solar Cells", *Solar Energy Materials and Solar Cells* 58, (1999) pp. 321-336.
- [17] A. Usami, "Theoretical Simulations of Optical Confinement in Dye-Sensitized Nanocrystalline Solar Cells," *Solar Energy Materials and Solar Cells*, 64 (2000) pp. 73-83.
- [18] X. Bi-Tao, Z. Bao-Xue, B. Jing, Z. Qing, L. Yan-Biao, C. Wei-Min and C. Jun, "Light Scattering of Nanocrystalline TiO₂ Film used in Dye-Sensitized Solar Cells", *Chin. Phys. Soc.* 17 [1019] (2008) pp. 3713-37.
- [19] L. Yang, Y. Lin, J. Jia, X. Xiao, X. Li, X. Zhou, "Light harvesting enhancement for DSSC by novel anode containing cauliflower-like TiO₂ spheres", *J. Power Sources*, 182 (2008) pp. 370-376.
- [20] L.E. McNeil and R.H. French, "Multiple Scattering from Rutile TiO₂ Particles", *Acta Mater.*, 48 (2000), pp. 4571-4576.
- [21] Q.F. Zhang, T.P. Chou, B. Russo, S.A. Jenekhe, and G.Z. Cao, "Light Scattering Enhanced Energy Conversion Efficiency in Hierarchically-Structure ZnO Dye Sensitized Solar Cells," *Advanced Functional Materials* 18, (2008) pp. 1654-1660.
- [22] X. Huang, P. Shen, B. Zhao, X. Feng, S. Jiang, H. Chen, H. Li, S. Tan, "Stainless steel mesh-based flexible quasi-solid dye-sensitized solar cells", *Sol Energy Materials & Solar Cells*, 94 (2010) pp. 1005-1010.
- [23] M. Song, D. Kim, S. Jo, D. Kim, "Enhancement of the photocurrent generation in dye-sensitized solar cell based on electrospun TiO₂ electrode by surface treatment", *Synthetic Metals* 155 (2005) pp. 635-638.
- [24] A. Gueye, "Novel TiO₂ Thick Film Microstructures for use in Dye Sensitized Solar Cells", MS Thesis, New Mexico Institute of Mining & Technology (2008).
- [25] M. Gratzel and G.P. Smestad, "Demonstrating electron transfer and nanotechnology: A natural dye-sensitized nanocrystalline energy converter", *J. Chem. Education*, 75 [6] (1998) pp. 752-759.
- [26] Margit J. Jensen and Paul A. Fuierer, "Low-temperature Preparation of Nanocrystalline Anatase Films Through a Sol-Gel Route", *J. of Sol-Gel Sci. & Tech.*, 39, (2006) pp. 229-233.
- [27] A. Varghese, "Synthesis of TiO₂ Coated Spheres and TiO₂ Particles by Spray Drying and their Photocatalytic Behavior", MS Thesis, New Mexico Institute of Mining & Technology (2008).
- [28] K.G. Chittibabu, J. He, L.A. Samuelson, S. Tripathy, J. Kumar, S. Balasubramanian, "Photovoltaic Cell" European Patent Publication # WO/2004/006292
- [29] B. Roy, S. Ahrenkiel, P. Fuierer, "Controlling the Size and Morphology of TiO₂ Powder by Molten and Solid Salt Synthesis," *J. Amer. Ceram. Soc.*, 91, [8] (2008) pp. 2455-2463.
- [30] B. Roy, P. Fuierer, S. Aich, "Synthesis of TiO₂ scaffold by a two-step bi-layer process using molten salt synthesis technique", *Powder Technology* (accepted).